

**A NEW METHODOLOGY FOR DETERMINATION OF  
LAMINAR BURNING VELOCITY IN A  
CYLINDRICAL VESSEL WITH FULL OPTICAL  
ACCESS USING CONSTANT VOLUME METHOD**

**VIKAS JANGIR**



**DEPARTMENT OF MECHANICAL ENGINEERING  
INDIAN INSTITUTE OF TECHNOLOGY DELHI**

**MAY 2023**

© Indian Institute of Technology Delhi (IITD), New Delhi, 2023

A NEW METHODOLOGY FOR DETERMINATION OF  
LAMINAR BURNING VELOCITY IN A CYLINDRICAL  
VESSEL WITH FULL OPTICAL ACCESS USING  
CONSTANT VOLUME METHOD

by

VIKAS JANGIR

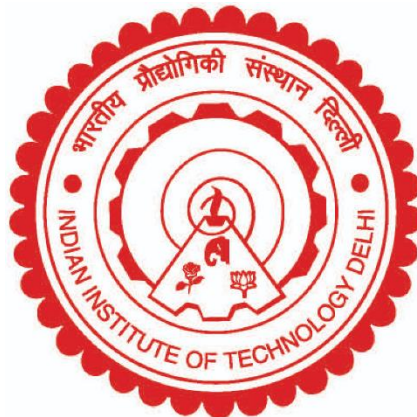
Department of Mechanical Engineering

submitted

in fulfillment of the requirements of the degree of

DOCTOR OF PHILOSOPHY

to the



INDIAN INSTITUTE OF TECHNOLOGY DELHI

MAY 2023

*Dedicated to*  
*My mother Mrs. Sushila Devi and father Mr. Rajendra Prasad Jangir,*  
*and*  
*to my wife Mrs. Kanak Lata and my daughter Anvi Jangir.*

## Certificate

This is to certify that the thesis entitled “**A New Methodology for Determination of Laminar Burning Velocity in a Cylindrical Vessel with Full Optical Access Using Constant Volume Method**” being submitted by **Mr. Vikas Jangir** (2016MEZ8547) to the Indian Institute of Technology Delhi, New Delhi, for the award of the degree of **Doctor of Philosophy** is a record of bonafide research work carried out by him under our supervision. The candidate has fulfilled the requirements for the submission of this research work for his thesis. In our opinion, this thesis has attained the standard needed for the award of a Ph.D. degree of this institute. The results contained in this thesis have not been submitted, in a part or in full, to any other university or institute for the award of any degree or diploma.

**Dr. Anjan Ray**

Professor

Department of Mechanical Engineering

Indian Institute of Technology, Delhi

**Dr. M. R. Ravi**

Professor

Department of Mechanical Engineering

Indian Institute of Technology, Delhi

## Acknowledgements

My first thanks go to the Almighty that I have come up to submit my thesis. The recent times have been a testing one, and I show my total devotion toward the Almighty for showing me the path at testing times.

My superiors deserve more than I can express in words. I am grateful to **Prof. Anjan Ray** and **Prof. M. R. Ravi** for their continuous support and guidance, which have shaped me into a skilled research scholar. Without their direction and support, this work would not have been possible. Their insight, expertise, and dedication to the highest standards have always motivated and inspired me. **Prof. Ravi's** advice and problem-solving skills never left me in a loop throughout my research efforts. He is an excellent researcher and a positive energy source who planted the seed of hope in me in every challenging circumstance I encountered while working on this work. **Prof. Anjan Ray** educated me in the field of combustion and provided me with the essential tools, without which this work could not have been accomplished. I aspire to adopt his systematic approach to resolving issues in the future.

In addition to my supervisors, I would like to thank the professors of my student research committee, **Prof. S. R. Kale**, **Prof. P.M.V. Subbarao**, **Prof. Mayank Kumar**, and **Prof. Divesh Bhatia**, for their insightful remarks and valuable feedback, which assisted me in shaping my research work into its current form.

I am also grateful to **Prof. Sangeeta Kohli** for helping me with uncertainty analysis for this work. I am also thankful to her for the invaluable life lessons I will take with me throughout my life.

Thanks to **Prof. Sudipto Mukherjee** for his help in designing my experimental setup. I would also like to thank all the instructors during the coursework. Their courses brought me a sense of commitment and clarity of thought.

Unparalleled support received from **Mukesh Sharma** and his team of **Nutech Electrinstruments India Pvt. Ltd.** during the fabrication of experimental rigs is gratefully acknowledged. Working with them during the setup fabrication was one of the best days. The credit provided by his workshop was beneficial and allowed me to approach them freely.

I acknowledge and thank **Mr. Ram Pal**, **Mr. Badri Prasad**, **Mr. Vipin Kakkar**, **Mr. Tulsi Ram**, **Mr. Jitendra Prasad**, **Mr. Roshan Lal**, **Mr. Bhagwan Das Sharma**, **Mr. Abhishek**

**Rana, Mr. Ayodhya Prasad, Ms. Rachna Joshi and Mr. Kamal Kumar** for many discussions and access to many machine tools in the IIT Delhi laboratories.

Seniors form an integral part of research career, and their company provides motivation and guidance. I would gratefully acknowledge **Dr. Abdul Rahman Khan** for seeding a sense of excellence in pressure measurements, image capture techniques and image processing tools. He also taught me CHEMKIN-PRO<sup>®</sup> simulation software. I am also thankful to **Dr. Vinod Kumar**, who always inspired me and taught me how to fight back during a challenging period.

I worked with a wonderful group of lab mates throughout my research work. I wish to thank **Dr. Abdul, Dr. Vinod, Dr. Zeba, Vipul, Anurag, Rahul, Santosh, Thirumoorthy, Manish, Saurabh, Ankit, Vikas, Abhay, Mayank, Hardik, Chaitanya** and **Rajesh**. Indirectly or directly, they were always active in my research and encouraged and supported me consistently. I would also like to thank **Mr. Saurabh Singh** for his help with my CFD simulations. I would also thank my friend since my M. Tech days, **Dr. Manish Raj** of Centre for Automotive Research & Tribology, for his company and support whenever required.

I cannot begin to express my gratitude to my family for all the love, support, encouragement, and prayers they have sent me throughout this journey. My parents, thank you for being my champions for the past 34 years. Your unconditional love and support have meant the world to me; I hope I have made you proud. To my siblings, **Laxmi Kant Jangir** and **Suman Jangir**, our friendly rivalry has motivated me to succeed. To my beloved grandparents, thank you for believing in me and all of your blessings.

My wife, **Kanak Lata**, deserves special recognition for the exceptional assistance and support she has provided me with, as well as for the encouragement she has given me during this pivotal period of my life. It is a great blessing to be the father of a lovely little girl (Anvi Jangir) who, no matter how stressful the day may have been, always makes me feel like a kid again and laugh. I owe a very particular thank you to my spouse's family for their unwavering support during my difficult times. A very special thank you to **Anu Jangir** for being in my life during my research work.

**Vikas Jangir**

## Abstract

Laminar burning velocity is a fundamental property of a fuel-air mixture at a given pressure, temperature and equivalence ratio. Many practical combustion appliance designs are based on the laminar burning velocity. It is also a strong candidate to validate or develop chemical kinetic models. The laminar burning velocity is also an important input in modelling turbulent premixed combustion in spark ignition engines. Therefore, its accurate measurement is necessary. The constant volume method is the only technique suitable for determining laminar burning velocity at engine-relevant thermodynamic conditions. Values of laminar burning velocity obtained by the conventional constant volume method suffer from the inaccuracies induced by the weak burned gas mass fraction model and the effect of flame stretch. Direct measurement of the flame radius along with pressure-time trace can result in accurate determination of laminar burning velocity in constant volume method. This motivates the present work to look closely at the constant volume method with a view to improve its accuracy/eliminate its weaknesses.

A spherical chamber would be the best choice for the constant volume method, as in such chambers, the flame remains spherical throughout the combustion. However, full optical access in a spherical chamber may produce lens effect due to the curvature of chamber walls, and would need an optical correction to get the correct flame radius. Spherical transparent chambers are also difficult to fabricate. The remedy for this is the use of flat optical windows. Use of flat optical windows in a spherical chamber restricts the useful range of the flame radius-time data. The other alternative is to use a cylindrical chamber with full flat optical windows. Such a combustion chamber gives direct visual access to the entire range of flame radii in the chamber, and can also help in detecting the onset of cellularity. A cylindrical combustion chamber with full optical access is also easy to fabricate.

Since the flame in a cylindrical vessel does not remain spherical throughout the period of propagation, the end-view radius obtained during the experiment cannot be used directly to compute the actual burned gas volume and flame surface area. The current work proposes a new methodology for determining accurate values of laminar burning velocity in a cylindrical vessel using constant volume method. A comprehensive numerical simulation of constant volume combustion in a cylindrical and spherical chamber is performed using computational fluid dynamics (CFD). Two normalized relations in a cylindrical vessel are developed using CFD simulations. The relationship obtained by numerical simulation between the normalized

radius of the end-view of the flame,  $(R_{f,end-view}/R_c)$  and the normalized burned gas volume  $(V_b/V_t)$  as well as the normalized flame surface area  $(A_f/A_t)$  in a cylindrical chamber is found to be purely geometric, and hence is independent of the fuel-air mixture and chamber size, so long as its aspect ratio is unity. Using these relationships, end-view of flame radius,  $R_{f,end-view}$ , can be mapped to correct burned gas volume and flame surface area in a cylindrical vessel of any size. Then, using burned gas volume, flame surface area and pressure-time trace, laminar burning velocity can be accurately calculated at each location of the flame without the need for a model for burned gas volume.

Firstly, the pressure-time trace and end-view flame radius obtained from numerical simulations, in combination with the mapping approach, are used to calculate laminar burning velocity using constant volume method. The obtained values of laminar burning velocity in a cylindrical vessel are identical to those obtained numerically in a spherical vessel. Second, using the proposed method, obtained values of laminar burning velocity are also corrected for flame stretch. A stretch-correction methodology requires the values of laminar burning velocity with different stretch rates at a given target state  $(p, T)$  of the mixture, for extrapolating the laminar burning velocity to zero stretch. Stretch-corrected values of laminar burning velocity obtained in a cylindrical vessel for a  $H_2 + O_2$  –diluent mixture at various equivalence ratios are in good agreement with those obtained in a spherical chamber.

The new methodology proposed using numerical simulation is demonstrated for experimental data for methane-air mixture. This starts with developing a new cylindrical combustion chamber of volume 10.86 litre with full optical access and heating arrangement. Using the experimentally recorded pressure-time trace, end-view of flame radius and mapping methodology, the laminar burning velocity for a stoichiometric methane-air mixture is determined using the constant volume method, and the results agree well with those of a previously published study. The present work also demonstrates the stretch-correction method, originally proposed by the author's research group [99], for methane-air flames for pressures up to 2.5 bar, for equivalence ratio 0.8 – 1.2. Thus, the present work significantly reduces the main drawbacks of the constant volume method, making the method a candidate for accurate determination of laminar burning velocity.

## सार

लैमिनार बर्निंग वेलोसिटी (LBV) दिए गए दाब, तापमान और समतुल्य अनुपात पर ईंधन-हवा के मिश्रण का एक मौलिक गुण है। कई दहन सम्बंधित उपकरणों की संरचना LBV पर आधारित है। इसका प्रयोग रासायनिक गतिज मॉडलों की पुष्टि या उन्हें विकसित करने के लिए किया जाता है। स्पार्क प्रज्वलन इंजन में होने वाले टर्बुलेंट प्रीमिक्सिड दहन की मॉडलिंग के लिए LBV का पता होना आवश्यक है। इसलिए, इसका सटीक मापन जरूरी है। इंजन-उपयुक्त ऊष्मा गतिकी स्थितियों में LBV को निर्धारित करने के लिए कांस्टेंट वॉल्यूम मेथड (CVM) एकमात्र तकनीक है। पारंपरिक CVM में जली हुई गैस का द्रव्यमान अंश निकालने के लिए जो मॉडल प्रयोग में लाया जाता है, उसकी कमियों के कारण और फ्लेम स्ट्रेच के प्रभाव से LBV का सही निर्धारण नहीं हो पाता। समय के साथ बदलते हुए दबाव के माप के अतिरिक्त फ्लेम त्रिज्या का माप भी किया जाए तो CVM के द्वारा LBV का सटीक निर्धारण किया जा सकता है। उपरोक्त वक्तव्य वर्तमान रिसर्च में CVM की सटीकता और उसकी कमियों का अवलोकन करने के लिए प्रेरित करता है।

CVM के लिए एक गोलाकार कक्ष सबसे अच्छा विकल्प है, क्योंकि ऐसे कक्षों में फ्लेम पूरे दहन के दौरान गोलाकार रहती है। हालाँकि, इस प्रकार के कक्ष में दीवारों की वक्रता के कारण लेंस प्रभाव उत्पन्न हो सकता है, जिसके कारण सटीक फ्लेम त्रिज्या प्राप्त करने के लिए ऑप्टिकल सुधार की आवश्यकता होगी। गोलाकार पारदर्शी कक्ष बनाना भी मुश्किल है। फ्लैट ऑप्टिकल विंडो का प्रयोग इन मुश्किलों को दूर कर सकता है। गोलाकार कक्ष में फ्लैट ऑप्टिकल विंडो का प्रयोग फ्लेम त्रिज्या-समय डेटा की उपयोगी सीमा को प्रतिबंधित करता है। पूर्ण फ्लैट ऑप्टिकल विंडो के साथ बेलनाकार कक्ष एक अन्य विकल्प है, और इसे बनाना भी आसान है। इस प्रकार का दहन कक्ष सम्पूर्ण फ्लेम त्रिज्या की दृश्यता और कोशकीय प्रभाव को पता लगाने में सहायक होता है।

बेलनाकार कक्ष में फ्लेम, प्रसार की अवधि के दौरान गोलाकार नहीं रहती। अतः प्रयोग के दौरान बेलनाकार के आधार की ओर से मापी हुई त्रिज्या का उपयोग जली हुई गैस की मात्रा और फ्लेम की सतह का क्षेत्रफल निकालने के लिए नहीं किया जा सकता। वर्तमान कार्य में CVM का प्रयोग करके बेलनाकार कक्ष में LBV के सटीक मान को निर्धारित करने के लिए एक नई पद्धति का प्रस्ताव रखा गया है। कम्प्यूटेशनल फ्लूइड डायनामिक्स (CFD) का उपयोग करके बेलनाकार और गोलाकार कक्षों में कांस्टेंट वॉल्यूम दहन का विस्तृत संख्यात्मक सिमुलेशन किया गया है। CFD सिमुलेशन का उपयोग करके बेलनाकार कक्ष में दहन के लिए दो सामान्यीकृत संबंध विकसित किए गए हैं। बेलनाकार कक्ष ( $L/D = 1$ ) में दहन की सिमुलेशन द्वारा, फ्लेम की सामान्यीकृत त्रिज्या ( $R_{f, endview}/R_c$ ) और जली हुई गैस की मात्रा

$(V_b/V_t)$  के बीच एवं फ्लेम की सामान्यीकृत त्रिज्या और फ्लेम की सतह के क्षेत्रफल ( $A_f/A_t$ ) के बीच जो संबंध निकाले गए हैं वे पूरी तरह से ज्यामिती पर आधारित हैं। अतः ये संबंध ईंधन-वायु मिश्रण और कक्ष के आकार पर निर्भर नहीं करते। इन संबंधों का उपयोग करके  $R_{f,endview}$  के किसी भी मान के लिए, किसी भी आकार के बेलनाकार कक्ष में जली हुई गैस की मात्रा और फ्लेम की सतह के क्षेत्रफल को प्राप्त किया जा सकता है। तदोपरांत, जली हुई गैस की मात्रा, फ्लेम की सतह के क्षेत्रफल और दाब-समय ट्रेस का उपयोग करके, जली हुई गैस का द्रव्यमान अंश निकाले बिना, LBV का सटीक निर्धारण किया जा सकता है।

सबसे पहले, संख्यात्मक सिमुलेशन से प्राप्त किये गए दाब-समय ट्रेस और  $R_{f,endview}$  का उपयोग करके CVM से LBV के मान निकाले गए हैं। बेलनाकार कक्ष में निकाले गए LBV के मान, गोलाकार कक्ष में निकाले गए मानों के बराबर है। इसके बाद, प्रस्तावित विधि का उपयोग करते हुए जो LBV के मान प्राप्त हुए हैं उनमें से फ्लेम स्ट्रेच के प्रभाव को दूर किया गया है। मिश्रण के दिए गए ताप और दाब ( $p, T$ ) पर प्राप्त किये गए LBV के मान से, फ्लेम स्ट्रेच के प्रभाव को दूर करने के लिए अलग-अलग फ्लेम स्ट्रेच के मानों के साथ LBV के मानों की आवश्यकता होती है, जिससे LBV के मान को फ्लेम स्ट्रेच के न होने की स्थिति के लिए निकाला जा सकता है। इस प्रकार से निकाले गए LBV के मान गोलाकार कक्ष में बिना फ्लेम स्ट्रेच के प्राप्त किये गए LBV के मानों के बराबर है।

प्रस्तावित की गयी पद्धति को मीथेन-वायु मिश्रण के प्रायोगिक आंकड़ों के लिए प्रदर्शित किया गया है। इस पद्धति का प्रयोग करने के लिए 10.86 लीटर का एक पारदर्शी बेलनाकार कक्ष बनाया गया है जिसे गर्म करने की भी व्यवस्था है। प्रयोग के दौरान प्राप्त किए गए दाब-समय ट्रेस,  $R_{f,endview}$  और विकसित किए गए संबंधों का उपयोग करके, CVM से स्टोइकियोमेट्रिक मीथेन-वायु मिश्रण की LBV के मान प्राप्त किये गए हैं, और प्राप्त किये गए मान पहले से प्रकाशित किये गए मानों के साथ अच्छी तरह से सहमति में हैं। वर्तमान कार्य में फ्लेम स्ट्रेच-सुधार विधि का प्रयोग करते हुए मीथेन-वायु मिश्रण के लिए 2.5 bar तक के दाब और समतुल्य अनुपात 0.8 - 1.2 के लिए स्ट्रेच रहित LBV के मान भी प्राप्त किये गए हैं। इस प्रकार, प्रस्तावित पद्धति CVM की सभी कमियों को पूरी तरह से समाप्त कर देती है, जिससे यह LBV के सटीक निर्धारण के लिए एक अच्छी विधि बन जाती है।

# Contents

<b>Certificate</b>	<b>i</b>
<b>Acknowledgement</b>	<b>ii</b>
<b>Abstract</b>	<b>iv</b>
<b>सार</b>	<b>vi</b>
<b>Contents</b>	<b>viii</b>
<b>List of Tables</b>	<b>xi</b>
<b>List of Figures</b>	<b>xii</b>
<b>Nomenclature</b>	<b>xvi</b>
<b>1 Introduction</b>	<b>1</b>
1.1 Measurement of laminar burning velocity	1
1.1.1 Stationary flame methods	2
1.1.2 Propagating/moving flame method	6
1.2 Objectives of the present work	9
1.3 Organization of the thesis	10
<b>2 Literature review on constant volume method</b>	<b>12</b>
2.1 Constant volume method without optical access	12
2.2 Constant volume method with full optical access to the chamber	17
2.2.1 Spherical chamber with full optical access	17
2.2.2 Cylindrical combustion chamber with full optical access	18
2.3 Effect of Stretch on laminar burning velocity obtained from constant volume method	19
2.4 Cellularity detection in constant volume method	25
2.5 Discussion of issues arising out of literature review	26
2.6 Gaps identified from the literature survey	27
2.7 Scope of the present work	28
<b>3 Design of experimental setup</b>	<b>30</b>
3.1 Selection of size of the combustion chamber	30
3.2 Selection of material for the combustion chamber	30
3.3 Design procedure for cylindrical constant volume combustion chamber	31
3.3.1 Components of the cylindrical combustion chamber	31
3.3.2 Design procedure and calculations	32
3.3.3 Final dimensions of the cylindrical combustion chamber	34
3.3.4 Summary description	34
3.4 Heater and controllers	35
3.5 Mixture preparation and ignition	35
3.5.1 Variable spark energy system to ignite the fuel-air mixtures	36
3.6 Measurement of pressure-time history	37
3.7 Imaging of flame front evolutions	37
3.8 Complete experimental setup	38

3.9	Experiment procedure	40
3.9.1	Post-processing of the experimental data	40
3.9.2	Laminar burning velocity using constant pressure method	41
3.9.3	Laminar burning velocity using constant volume method	41
3.9.3.1	Stretch-correction on measured laminar burning velocity	42
3.9.4	Uncertainty evaluation	42
3.10	Validation of newly developed setup using constant pressure method	43
<b>4</b>	<b>Determining laminar burning velocity from pressure and flame volume-surface area histories – a numerical study</b>	<b>45</b>
4.1	Methodology	45
4.2	Numerical model	46
4.3	Grid independence	48
4.4	Tracking of the flame	49
4.5	Results and discussion	50
4.5.1	Flame volume, surface area and flame radii	50
4.5.2	Scaling with size of combustion chamber	54
4.6	Mapping flame end-view radius to burned gas volume and flame surface area in a cylindrical chamber	54
4.7	Demonstration of the proposed method using experimental data for a stoichiometric Methane-air flame	60
4.8	Conclusions	63
<b>5</b>	<b>Stretch-correction in constant volume method using cylindrical vessel – a numerical study</b>	<b>64</b>
5.1	Method of stretch-correction	65
5.2	Stretch-correction for hydrogen flames using numerical simulation	66
5.2.1	Methodology	66
5.2.2	Numerical model	66
5.2.3	Stretch-correction of calculated laminar burning velocity	68
5.3	Validation of Stretch-Corrected laminar burning velocity Obtained by constant volume method in a cylindrical vessel	72
5.4	Conclusions	77
<b>6</b>	<b>Stretch-correction in constant volume method using cylindrical vessel– experimental study</b>	<b>78</b>
6.1	Initial conditions of fuel-air mixture	78
6.2	Determination of laminar burning velocity using constant volume method	80
6.3	Stretch-correction on laminar burning velocity	80
6.4	Determination of laminar burning velocity using constant pressure method	84
6.5	Stretch-corrected laminar burning velocity of methane-hydrogen-air mixtures at elevated pressures and temperature	86
6.6	Conclusions	90
<b>7</b>	<b>Conclusions and scope of further study</b>	<b>91</b>
7.1	Conclusions	91
7.2	Major contributions of present work	93
7.3	Scope of future work	93

<b>Appendices</b>	<b>95</b>
<b>A Design of a cylindrical combustion chamber with full optical access</b>	<b>96</b>
A.1 Thickness of the cylindrical tube	96
A.2 Thickness of the inner flange	98
A.3 Thickness of the optical window	99
A.4 Thickness of the outer flange	103
A.5 Number of M20 bolts and pretension required in each bolt with a gasket	108
A.6 The sealing of the flanges with O-ring [127]	108
A.7 Groove dimensions based on the O Ring dimensions	110
A.8 Bolt pretension required to seal the flanges with an O-ring	111
<b>B Uncertainty Calculation</b>	<b>114</b>
B.1 Systematic uncertainty in equivalence ratio	114
B.2 Systematic uncertainty in time	115
B.3 Systematic uncertainty in flame radius	115
B.4 Uncertainty in flame surface area	116
B.5 Uncertainty in burned gas volume	116
B.6 Uncertainty in the temporal derivative of the burned gas volume	116
B.7 Uncertainty in chamber pressure measurement	116
B.8 Uncertainty in laminar burning velocity determination	117
<b>References</b>	<b>118</b>
<b>List of Publications</b>	<b>130</b>
<b>Bio-Data</b>	<b>131</b>

## List of Tables

2.1	Range of pressure, temperature and equivalence ratio for power-law correlations	15
3.1	Input parameters to design cylindrical combustion chamber	32
3.2	Different parameters of a cylindrical combustion chamber for a 50 bar design pressure	33
3.3	Final dimensions of various parameters of combustion chamber	34
4.1	Parameters of the model	48
4.2	Different combustible mixtures	55
A.1	Input Parameters for PTFE Gasket	107
A.2	Input parameters for class 8.8 bolts (Medium carbon steel: Quenched and tempered)	107
A.3	Input parameters for SS304	109
A.4	Input parameters for Fused Quartz GE124	109
A.5	Specifications of the O-ring	110
A.6	Groove dimensions	111

## List of Figures

1.1	Sketch of Bunsen burner flame and flow conditions [7]	2
1.2	Schematic of the stagnation flow field with flat flames for the stagnation flow method	4
1.3	Sketch of flat flame burner using heat flux method [17]	5
2.1	Variation of laminar burning velocity for methane-air mixture with pressures and temperatures along a $p - T$ curve of isentropic compression. Symbols: calculated using power-law correlations (Iijima et al. [60]; Hill and Hung [61]; Stone et al. [53]; Elia et al. [62]; Han et al. [63]; Marshall et al. [64]; Hinton et al. [65]; Reyes et al. [66]; Wang et al. [33]); solid line represents the temperatures corresponding to pressures	17
2.2a	Comparison of stretch-free and stretched values of laminar burning velocity of methane-air flame. Line represents the stretch-free values of laminar burning velocity using CPM [79]; Symbols represent the stretched values of laminar burning velocity obtained by power-law correlation (Iijima et al. [60]; Stone et al. [53]; Elia et al. [62]; Marshall et al. [64]; Reyes et al. [66]; Hinton et al. [65])	21
2.2b	Comparison of stretch-free and stretched values of laminar burning velocity methane-air flame. Line represents the stretch-free values of laminar burning velocity using CPM [80]; Symbols represent the stretched values of laminar burning velocity obtained by power-law correlation (Iijima et al. [60]; Stone et al. [53]; Elia et al. [62]; Marshall et al. [64]; Reyes et al. [66]; Hinton et al. [65])	22
2.2c	Comparison of stretch-free and stretched values of laminar burning velocity methane-air flame. Line represents the stretch-free values of laminar burning velocity using CPM [65]; Symbols represent the stretched values of laminar burning velocity obtained by power-law correlation (Iijima et al. [60]; Stone et al. [53]; Elia et al. [62]; Marshall et al. [64]; Reyes et al. [66]; Hinton et al. [65])	23
2.2d	Comparison of stretch-free and stretched values of laminar burning velocity methane-air flame. Line represents the stretch-free values of laminar burning velocity using diverging channel method [81]; Symbols represent the stretched values of laminar burning velocity obtained by power-law correlation (Iijima et al. [60]; Elia et al. [62]; Marshall et al. [64]; Hinton et al. [65])	24
3.1	Sketch of combustion chamber	31
3.2	Sectional view of the cylindrical combustion chamber	34
3.3	Variable spark energy system circuit diagram	37
3.4	Typical evolutions of an end-view of flame radius in the cylindrical chamber for the methane-air flame	38
3.5	Sketch of layout of experimental setup	39
3.6	Typical chamber pressure evolution as a function of time for methane-air flame	41
3.7	Laminar burning velocity for methane-air flames at 1 bar and 300 K. Symbols: experiments (Hassan et al. [108]; Rozenchan et al. 2002 [109]; Lowery et al. [110]; Halter et al. 2010 [104]; Park et al. 2011 [111]; Akram et al. 2013 [112]; Goswami et al. 2013 [21]; Hu et al. [80]); Current experimental results are shown as solid lines with symbols	43

4.1	Computational domain for 0.524 L cylindrical (1:1) and spherical vessels	46
4.2a	Pressure-time trace	49
4.2b	Pressure rise rate-time trace	49
4.3	Flame position at different isotherm for 0.524 L spherical case	50
4.4	Variation of chamber pressure	51
4.5	Variation of pressure rise rate	51
4.6a	Burned gas volume versus pressure in different vessels	52
4.6b	Flame surface area versus pressure in different vessels	53
4.6c	Evolution of flame surface contours (in a plane parallel to the length of the cylindrical vessel) for a flame in spherical (solid lines) and cylindrical vessels (dashed lines) of size 0.524 L	53
4.7	Normalized burned volume versus pressure in different vessels	54
4.8a	Variation of normalized burned gas volume with normalized end-view flame radius	56
4.8b	Variation of normalized flame surface area with normalized end-view flame radius	56
4.9	Laminar burning velocity versus pressure for $H_2 + O_2 + 7He$ mixture in a 0.524 L cylindrical and spherical vessel (initial condition: $p_i = 1.01$ bar; $T_i = 300$ K; $\phi = 3.0$ )	57
4.10	LBV versus pressure for 0.524 L spherical vessel for $H_2 + O_2 + 7He$ mixture (initial condition: $p_i = 1.01$ bar $T_i = 300$ K; $\phi = 3.0$ )	58
4.11	Percentage difference in flame radius computed using burned gas mass fraction models and compared to accuracy with actual flame radius. (initial condition: $p_i = 1.01$ bar; $T_i = 300$ K; $\phi = 3.0$ )	58
4.12a	Sensitivity analysis of the flame speed with (+2) % perturbation to the flame radius ( $R_f$ ), the pressure ( $p$ ) and the unburned gas heat capacities ratio ( $\gamma_u$ )	59
4.12b	Sensitivity analysis of the flame speed with (-2) % perturbation to the flame radius ( $R_f$ ), the pressure ( $p$ ) and the unburned gas heat capacities ratio ( $\gamma_u$ )	60
4.13	End-view of flame front evolution for stoichiometric methane-air mixture (initial condition: $p_i = 1$ bar; $T_i = 305$ K; $\phi = 1.0$ )	61
4.14	Laminar burning velocity of stoichiometric methane-air mixture (initial condition: $p_i = 1$ bar; $T_i = 305$ K; $\phi = 1.0$ ). Symbols represent results using CHEMKIN-PRO and power-law correlation (Hinton et al. 2018 [65]; Elia et al. 2001 [62]; Stone et al. 1998 [53]); solid lines represent the experimental results	62
5.1a	Initial conditions of Hydrogen mixtures with ( $O_2 + 7He$ ) along an isentrope. (a) $P_i = 1.01325$ bar, $T_i = 300$ K, $\phi = 3.0$ ; (b) $P_i = 1.01325$ bar, $T_i = 300$ K, $\phi = 3.5$ ; and (c) $P_i = 1.01325$ bar, $T_i = 300$ K, $\phi = 4.0$	66
5.1b	Pressure-time trace for Hydrogen mixtures with ( $O_2 + 7He$ ). Solid lines for a spherical vessel; dashed lines for a cylindrical vessel	67
5.1c	Pressure-time trace for Hydrogen mixtures with ( $O_2 + 7He$ ). Solid lines for a spherical vessel; dashed lines for a cylindrical vessel	67
5.1d	Pressure-time trace for Hydrogen mixtures with ( $O_2 + 7He$ ). Solid lines for a spherical vessel; dashed lines for a cylindrical vessel	68

5.2a	Calculated Laminar burning velocity as a function of pressure and corresponding isentropic compression temperature for Hydrogen mixtures with ( $O_2 + 7He$ ) at $\phi = 3.0$	68
5.2b	Calculated Laminar burning velocity as a function of pressure and corresponding isentropic compression temperature for Hydrogen mixtures with ( $O_2 + 7He$ ) at $\phi = 3.5$	69
5.2c	Extrapolation of stretched laminar burning velocity calculated using constant volume method for Hydrogen flames in ( $(O_2 + 7He)$ ; $\phi = 3.0$ ) at $p = 2.5 \text{ bar}$ ; $T = 405.73 \text{ K}$	69
5.2d	Extrapolation of stretched laminar burning velocity calculated using constant volume method for Hydrogen flames in ( $(O_2 + 7He)$ ; $\phi = 3.5$ ) at $p = 2.5 \text{ bar}$ ; $T = 404.32 \text{ K}$	70
5.2e	Extrapolation of stretched laminar burning velocity calculated using constant volume method for Hydrogen flames in ( $(O_2 + 7He)$ ; $\phi = 4.0$ ) at $p = 2.5 \text{ bar}$ ; $T = 403.06 \text{ K}$	70
5.3a	The stretch-corrected laminar burning velocity for hydrogen flames in ( $(O_2 + 7He)$ ; $\phi = 3.0$ ) at different pressures and corresponding isentropic compression temperatures	71
5.3b	The stretch-corrected laminar burning velocity for hydrogen flames in ( $(O_2 + 7He)$ ; $\phi = 3.5$ ) at different pressures and corresponding isentropic compression temperatures	71
5.3c	The stretch-corrected laminar burning velocity for hydrogen flames in ( $(O_2 + 7He)$ ; $\phi = 4.0$ ) at different pressures and corresponding isentropic compression temperatures	72
5.4	Comparison of stretch-free values of laminar burning velocity for Hydrogen-air flames at 1 bar and 300 K. Symbols: experiments (Sabard et al. [119]; Kuznetsov et al. [120]; Burke et al. [67]; Dayma et al. [121]); line: calculations using CHEMKIN	73
5.5	Comparison of stretch-free values of laminar burning velocity for Hydrogen-air flames at 1 bar and 300 K. Symbol: experiment (Aung et al. [122]); line: calculations using CHEMKIN	74
5.6	Variation of laminar burning velocity with pressure (corresponding isentropic compression temperature), of ( $H_2 + O_2 + 7He$ ) mixture	74
5.7a	Variation of laminar burning velocity with pressure (corresponding isentropic compression temperature on secondary horizontal axis), of ( $H_2 + O_2 + 7He$ ) mixture at $\phi = 3.0$	75
5.7b	Variation of laminar burning velocity with pressure (corresponding isentropic compression temperature on secondary horizontal axis), of ( $H_2 + O_2 + 7He$ ) mixture at $\phi = 3.5$	76
5.7c	Variation of laminar burning velocity with pressure (corresponding isentropic compression temperature on secondary horizontal axis), of ( $H_2 + O_2 + 7He$ ) mixture at $\phi = 4.0$	76
6.1	Initial conditions of Methane-air mixtures along an isentrope. (a) for lean mixture ( $\phi = 0.8$ ); (b) for stoichiometric mixture ( $\phi = 1.0$ ); and (c) for rich mixture ( $\phi = 1.2$ )	78

6.2	Evolution of the end-view of flame radius in the cylindrical chamber for the methane-air flame	79
6.3	Extrapolation of stretched laminar burning velocity using four and five data points	81
6.4	Linear extrapolation for stretch-correction of lean ( $\phi = 0.8$ ), stoichiometric ( $\phi = 1.0$ ), and rich ( $\phi = 1.2$ ) methane-air flames at target states of $p = 1.5$ bar and $p = 2.0$ bar	82
6.5	The stretch-corrected laminar burning velocity for the methane-air mixture at different pressures and temperatures along the $p - T$ curve of isentropic compression	83
6.6	Variation of stretched and stretched-corrected laminar burning velocity obtained using constant volume method at different pressure ratios for methane-air flames	84
6.7	Extrapolation of burned flame speed for rich Methane-air flames ( $\phi = 1.2$ )	85
6.8	Laminar burning velocity of methane-air mixture using constant pressure method	86
6.9	The effect of initial mixture temperature on the laminar burning velocity of methane-air mixture obtained using constant pressure method	87
6.10	Effect of flame cellularity for a (a) stoichiometric and (b) rich methane-air mixture on the values of laminar burning velocity at various pressures and corresponding temperatures of the mixture along their $p - T$ curve of isentropic compression	88
6.11	Laminar burning velocity of methane-hydrogen mixture over various pressures and temperatures along a $p - T$ curve of isentropic compression (initial condition: $p_i = 1 \text{ bar}$ ; $T_i = 289 \text{ K}$ ; $\phi = 1.0$ )	89
A.1	Sketch of a cylindrical tube with inner flange	96
A.2	Sectional view of the cylindrical tube with an inner flange	97
A.3	Sketch of the fused Quartz window	100
A.4	Fused Quartz window fixed at the edges with uniformly distributed pressure	100
A.5	Fused quartz window simply supported at the edge with uniformly distributed pressure	101
A.6	Outer flange fixed at the bolt circle diameter with uniformly distributed pressure from the inner diameter to bolt circle diameter	103
A.7	Sectional view of supporting and outer flanges	105
A.8	Sketch of gasket	106
A.9	Preload in each bolt	112

## Nomenclature

### Abbreviations

1 – D	One Dimensional
PLC	Power-law Correlation
EGR	Exhaust Gas Re-circulation
CPM	Constant Pressure Method
CVM	Constant Volume Method
LBV	Laminar Burning Velocity
HTDR	Hybrid ThermoDynamic-Radiation
CFD	Computational Fluid Dynamics
ASME	American Society of Mechanical Engineers
TOF	Theory of Failure
PID	Proportional Integral Derivative
CCS	Control Center Series
MIE	Minimum Ignition Energy
IGBT	Insulated-gate Bipolar Transistor
PISO	Pressure-implicit Splitting of Operators

### Greek Letters

$\alpha$	Temperature Exponent
$\beta$	Pressure Exponent
$\Phi$	Equivalence Ratio
$\theta$	Half Cone Angle
$\gamma$	Specific Heats Ratio
$\gamma_u$	Unburned Mixture Specific Heats Ratio
$\gamma_b$	Burned Gas Specific Heats Ratio
$\rho_u$	Unburned Mixture Density
$\rho_b$	Burned Mixture Density
$\sigma_a$	Axial Stress
$\sigma_r$	Radial Stress
$\sigma_t$	Tangential Stress

$\sigma_{ys}$	Yield Strength
$\sigma_{bending}$	Bending Strength
$\tau$	Shear Stress
$K$	Flame Stretch Rate
<b>Symbols</b>	
$A_f$	Flame Surface Area
$A_t$	Total Inner Surface Area
$D_{bolt\ circle}$	Bolt Circle Diameter
$D_{inner\ dia\ of\ groove}$	Inner Dia of Groove
$D_i, inner\ flange$	Inner Dia of Inner Flange
$D_i, pipe$	Inner Dia of Pipe
$D_i, supporting\ flange$	Inner Dia of Supporting Flange
$D_i, outer\ flange$	Inner Dia of Outer Flange
$D_g$	Dia of Fused Quartz Glass Exposed to Pressure
$L$	Litre
$\dot{m}$	Mass Flow Rate
$m_u$	Unburned Mixture Mass
$p$	Pressure
$p_i$	Initial Pressure
$p_e$	End Pressure/Maximum Pressure
$R$	Spherical Chamber Radius
$R_c$	Cylindrical Chamber Radius
$R_f$	Spherical Flame Radius
$R_{f,end-view}$	End-View Flame Radius
$R_i$	Inner Radius of Cylindrical Vessel
$R_o$	Outer Radius of Cylindrical Vessel
$S_b$	Stretched Flame Speed
$S_b^0$	Unstretched Flame Speed
$S_u$	Stretched Laminar Burning Velocity

$S_u^0$	Unstretched Laminar Burning Velocity
$t$	Time
$T$	Temperature
$t_{cc}$	Combustion Chamber Wall Thickness
$t_{glass}$	Fused Quartz Plate Thickness
$T_i$	Initial Temperature
$t_{inner\ flange}$	Inner Flange Thickness
$t_{outer\ flange}$	Outer Flange Thickness
$U_g$	Unburned Fuel-air Mixture Velocity
$V_b$	Burned Gas Volume
$V_t$	Combustion Chamber Total Volume
$v_u$	Unburned Mixture Specific Volume
$x$	Burned Gas Mass Fraction

**Subscripts**

$b$	Burned
$i$	Initial
$u$	Unburned